Swelling of *p*H-sensitive hydrogels

A. D. Drozdov[1,2,*] and J. deClaville Christiansen[2]

[1]*Center for Plastics Technology, Danish Technological Institute, Gregersensvej 7, DK-2630 Taastrup, Denmark*

[2]*Department of Mechanical and Manufacturing Engineering, Aalborg University, Fibigerstraede 16, DK-9220 Aalborg, Denmark*

(Received 1 October 2014; revised manuscript received 13 December 2014; published 17 February 2015)

A model is derived for the elastic response of polyelectrolyte gels subjected to unconstrained and constrained swelling. A gel is treated as a three-phase medium consisting of a solid phase (polymer network), solvent (water), and solutes (mobile ions). Transport of solvent and solutes is modeled as their diffusion through the network accelerated by an electric field formed by ions and accompanied by chemical reactions (dissociation of functional groups attached to the chains). Constitutive equations (including the van't Hoff law for ionic pressure and the Henderson-Hasselbach equation for ionization of chains) are derived by means of the free energy imbalance inequality. Good agreement is demonstrated between equilibrium swelling diagrams on several *p*H-sensitive gels and results of simulation. It is revealed that swelling of polyelectrolyte gels is driven by electrostatic repulsion of bound charges, whereas the effect of ionic pressure is of secondary importance.

DOI: 10.1103/PhysRevE.91.022305 PACS number(s): 82.33.Ln, 82.70.Gg, 83.80.Kn, 82.35.Rs

I. INTRODUCTION

This paper deals with constitutive modeling of the elastic response of polyelectrolyte gels and numerical simulation of the influence of *p*H of water on their unconstrained and constrained swelling. Hydrogels are three-dimensional networks of polymer chains linked by covalent bonds, physical cross-links, hydrogen bonds, van der Waals interactions, and crystallite associations [1]. When a gel is brought into contact with water, it swells, retaining structural integrity and the ability to withstand large deformations. Stimulus-sensitive hydrogels form an important class of gels whose equilibrium degree of swelling and kinetics of water uptake are strongly affected by external stimuli (temperature, *p*H, ionic strength, electric field, light, and enzymes) [2–4].

Functional groups attached to polymer chains in *p*H-responsive gels dissociate into mobile ions and bound charges under swelling. Depending on the charge of ionized groups, anionic, cationic, and ampholytic gels are distinguished. For definiteness, we analyze water uptake by anionic gels.

Although studies on swelling of polyelectrolyte gels have a long history, they have recently became a focus of attention, as these materials demonstrate the potential for a wide range of "smart" applications including biomedical devices, drug delivery carriers, scaffolds for tissue engineering, filters and membranes for selective diffusion, sensors for online process monitoring, soft actuators, and optical systems [5–8].

Comparison of observations on neutral and polyelectrolyte hydrogels reveals that (i) ionic gels demonstrate a faster kinetics of water uptake, and (ii) their equilibrium degree of swelling exceeds that of neutral gels. The former feature is conventionally explained by electro-osmosis: an electric field formed by mobile ions accelerates their flow, which, in turn, induces an increase in speed of water molecules with which these ions are associated. The larger equilibrium water uptake is described by two mechanisms: (i) development of ionic pressure (an excess pressure induced by the difference in concentrations of ions inside a specimen versus in the surrounding water bath) and (ii) electrostatic repulsion of bound charges. Although there are no doubts regarding the importance of both mechanisms for swelling of polyelectrolyte gels, analysis of experimental data is traditionally grounded on the assumption that ionic pressure plays the key role, while the effect of interaction between bound charges is subordinate (in a number of studies it is referred to in order to explain discrepancies between observations and their predictions; see [9] for a discussion). This approach may be explained by the absence of simple expressions for the energy of electrostatic repulsion of bound changes to be employed in fitting observations [10–13].

The objective of this study is to develop constitutive equations for the elastic response of polyelectrolyte gels that take into account both mechanisms of water uptake, to apply these relations to the analysis of experimental swelling diagrams, and to demonstrate that electrostatic repulsion of bound charges may greatly exceed ionic pressure.

The history of constitutive modeling of polyelectrolyte gels goes back to the 1950s. This subject recently attracted substantial attention when it was confirmed by observations that equilibrium water uptake by *p*H-sensitive gels is strongly affected by geometrical constraints, which requires an adequate description of stresses under arbitrary three-dimensional deformations accompanied by swelling [14,15]. Constitutive equations for the mechanical behavior of *p*H-sensitive gels under swelling have recently been derived in [16–26], to mention a few. To avoid complications induced by coupling of diffusion of species, evolution of the electric field, dissociation reactions, and development of stresses, most of these studies are based on a semithermodynamic approach. According to this concept, an explicit expression is introduced for the free energy density of a hydrogel, and stress-strain relations and chemical potentials of water molecules and ions are derived by differentiation of this expression with respect to appropriate arguments (which implies that the Maxwell stresses driven by the self-energy of the electric field are neglected [19]). When the electrochemical potentials are applied to describe the kinetics of swelling, an unavoidable arbitrariness appears in the

*add@teknologisk.dk

extension of the Henderson-Hasselbach equation to hydrogels [27] (due to the absence of thermodynamic restrictions on the rate of dissociation of functional groups) and the van't Hoff formula for ionic pressure (because simplified expressions for the specific free energy do not involve appropriate terms).

The aim of this work is to reveal that these apparent inconsistencies disappear within a strictly thermodynamic approach based on the free energy imbalance inequality. In particular, it is shown that (i) the classical form of the Henderson-Hasselbach equation is applicable to polyelectrolyte gels, and the corresponding dissociation constant can be expressed by means of the chemical potential of hydroxide ions and the difference in chemical potentials between noncharged and charged functional groups, whereas (ii) ionic pressure obeys the van't Hoff formula when the equilibrium degree of swelling is large compared with unity.

The constitutive model is grounded in the following assumptions: (i) the reference (stress-free) state of the equivalent polymer network differs from its initial state [15], (ii) transformation of the initial configuration of an isotropic network into its reference configuration is treated as volume expansion with a coefficient that increases linearly with the degree of ionization of chains, and (iii) the strain energy density of the equivalent network is a function of the principal invariants of the Cauchy-Green tensor for transition from the reference state into the actual state. Although application of these hypotheses to polyelectrolyte gels appears to be novel, the pronounced similarity between our approach and conventional concepts in finite thermoelasticity (with degree of ionization playing the role of temperature increment) should be mentioned.

The exposition is organized as follows. Constitutive equations for a polyelectrolyte gel under an arbitrary three-dimensional deformation accompanied by swelling are developed in Sec. II (technical details are reported in the Appendix). These relations are applied to the analysis of observations under unconstrained and constrained swelling in Sec. III. Concluding remarks are formulated in Sec. IV.

II. CONSTITUTIVE MODEL

A polyelectrolyte gel is treated as a three-phase medium consisting of a solid phase (polymer network), solvent (water), and solutes (mobile ions). Transport of solvent and solutes is modeled as their diffusion through the network accompanied by chemical reactions (dissociation of functional groups attached to chains) and accelerated by an electric field formed by mobile and fixed ions.

A. Chemical reactions

Due to self-ionization of water in the bath,

$$2H_2O \rightleftarrows H_3O^+ + OH^-, \tag{1}$$

it contains positively charged hydronium ions H_3O^+ (hydroxide ions H^+ associated with water molecules) and negatively charged hydroxyl radicals OH^-. Concentrations of positive and negative ions are characterized by

$$p\mathrm{H} = -\log_{10}[H^+], \quad p\mathrm{OH} = -\log_{10}[OH^-], \tag{2}$$

where $[H^+]$ and $[OH^-]$ stand for the molar fractions of H^+ and OH^- ions. In thermodynamic equilibrium, pH and pOH obey the equality

$$p\mathrm{H} + p\mathrm{OH} = p\mathrm{K_w}, \tag{3}$$

where $\mathrm{K_w}$ denotes the water ionization constant, and $p\mathrm{K_w} = -\log_{10}\mathrm{K_w}$, with $p\mathrm{K_w} = 14$ at room temperature. The electroneutrality condition for deionized water $[H^+] = [OH^-]$ together with Eq. (3) implies that $p\mathrm{H} = 7$.

To alter the pH of water, hydrochloric acid or sodium hydroxide is conventionally added to the bath. To obtain acidic conditions with $p\mathrm{H} < 7$ (which are the focus of this study), strongly acidic HCl is immersed, which dissociates entirely into H^+ ions (associated with water molecules) and Cl^- ions:

$$H_2O + HCl \rightleftarrows H_3O^+ + Cl^-. \tag{4}$$

When a polyelectrolyte chain is immersed in a bath, some functional groups in the chain dissociate, which results in the formation of bound charges attached to the chain and mobile ions dissolved in water. Presuming bound charges to be monovalent and negative, we model this process as dissociation of carboxyl groups:

$$H_2O + COOH \rightleftarrows H_3O^+ + COO^-. \tag{5}$$

Denote by n_1 the number of ionized groups COO^-; by n_2, the number of nonionized groups COOH; and by $n = n_1 + n_2$, the number of functional groups per chain. The degree of ionization α is defined as the ratio of the number of ionized groups to the total number of functional groups per chain:

$$\alpha = \frac{n_1}{n}. \tag{6}$$

Denote by $\bar{c}$, $\bar{c}_{H^+}$, $\bar{c}_{OH^-}$, and $\bar{c}_{Cl^-}$ the concentrations (number of species per unit volume) of water molecules, hydroxide ions, hydroxyl radicals, and chloride ions in the bath. The molar fractions of ions are connected with their concentrations by the relations

$$[H^+] = \kappa\frac{\bar{c}_{H^+}}{\bar{c}}, \quad [OH^-] = \kappa\frac{\bar{c}_{OH^-}}{\bar{c}}, \quad [Cl^-] = \kappa\frac{\bar{c}_{Cl^-}}{\bar{c}}, \tag{7}$$

where $\kappa = 1000/18$ represents the molarity of water.

With reference to the conventional approach to the analysis of water uptake by polyelectrolyte gels, the bath is treated in what follows as an infinite reservoir containing solvent (water) and solutes (mobile ions) at fixed concentrations; fast reactions (1) and (4) are disregarded in the free energy imbalance inequality; and reaction (5) is described without accounting for the association of mobile ions with water molecules. An explicit account of self-ionization of water inside a gel leads to a slight modification of reaction-diffusion equations [28] but does not affect the conditions of equilibrium swelling.

B. Macrodeformation of a hydrogel

Macrodeformation of a gel coincides with macrodeformation of its polymer network. For definiteness, the initial state is chosen to coincide with that of the undeformed dry specimen. Transformation of the initial configuration into the actual configuration is determined by the deformation gradient

F. The Cauchy-Green tensors for macrodeformation read

$$\mathbf{B} = \mathbf{F}\cdot\mathbf{F}^{\top}, \quad \mathbf{C} = \mathbf{F}^{\top}\cdot\mathbf{F}, \tag{8}$$

where the center dot stands for the inner product, and $\top$ denotes transpose.

The volume element in the actual configuration $\mathrm{d}v$ is expressed by means of the volume element in the initial configuration $\mathrm{d}V$ as

$$\mathrm{d}v = J\mathrm{d}V, \tag{9}$$

where

$$J = \det\mathbf{F}. \tag{10}$$

The surface element $\mathbf{n}\mathrm{d}a$ with unit normal $\mathbf{n}$ in the actual configuration is connected with the surface element $\mathbf{N}\mathrm{d}A$ with unit normal $\mathbf{N}$ in the initial configuration by the equation

$$\mathbf{n}\mathrm{d}a = J\mathbf{F}^{-\top}\cdot\mathbf{N}\mathrm{d}A = J\mathbf{N}\cdot\mathbf{F}^{-1}\mathrm{d}A. \tag{11}$$

Denote by C the concentration of water molecules in the actual state per unit volume in the initial configuration. Disregarding volume changes in a hydrogel driven by the presence of solutes and adopting the molecular incompressibility condition, we write

$$J = 1 + Cv, \tag{12}$$

where v stands for the characteristic volume of a water molecule. Neglecting clustering of water molecules, we estimate v from the condition

$$\bar{c}v = 1. \tag{13}$$

Let C_{H^+}, C_{OH^-}, and C_{Cl^-} be the concentrations of hydroxide ions H^+, hydroxyl radicals OH^-, and chloride ions Cl^- in the actual state per unit volume in the initial configuration. According to Eq. (9), the concentrations of water molecules and mobile ions per unit volume in the actual configuration read

$$c = \frac{C}{J}, \quad c_{\mathrm{H}^+} = \frac{C_{\mathrm{H}^+}}{J}, \quad c_{\mathrm{OH}^-} = \frac{C_{\mathrm{OH}^-}}{J}, \quad c_{\mathrm{Cl}^-} = \frac{C_{\mathrm{Cl}^-}}{J}. \tag{14}$$

Denote by M the number of chains in the equivalent polymer network, and by $C_b = Mn$ the concentration of functional groups attached to chains. The concentration of bound charges per unit volume in the initial configuration reads $C_{b^-} = \alpha C_b$.

C. Electric field

Denote by Φ the potential of the electric field formed by mobile ions and bound charges. The electric-field vectors, $\mathbf{e}$ and $\mathbf{E}$, in the actual and initial states are given by

$$\mathbf{e} = -\nabla\Phi, \quad \mathbf{E} = -\nabla_0\Phi, \tag{15}$$

where ∇ and ∇_0 are the gradient operators in the actual and initial configurations. A gel is modeled as a linear dielectric material whose electric displacement vector in the actual state reads

$$\mathbf{h} = \epsilon\mathbf{e}, \tag{16}$$

where the constant $\epsilon = \epsilon_0\epsilon_{\mathrm{r}}$ stands for the electric permittivity, ϵ_0 is the vacuum permittivity, and ϵ_{r} is the relative permittivity. It follows from Eqs. (15) and (16), and the chain rule for differentiation,

$$\nabla_0\Phi = \nabla\Phi\cdot\mathbf{F} = \mathbf{F}^{\top}\cdot\nabla\Phi, \tag{17}$$

that

$$\mathbf{E} = \mathbf{e}\cdot\mathbf{F} = \mathbf{F}^{\top}\cdot\mathbf{e}, \quad \mathbf{h} = \epsilon\mathbf{E}\cdot\mathbf{F}^{-1} = \epsilon\mathbf{F}^{-\top}\cdot\mathbf{E}. \tag{18}$$

Let Ω be an arbitrary domain with boundary $\partial\Omega$ in the initial state. Their images upon transition into the actual configuration are denoted ω and $\partial\omega$. The Gauss law for a dielectric medium reads

$$\int_{\partial\omega}\mathbf{h}\cdot\mathbf{n}\mathrm{d}a = \int_{\omega} r\mathrm{d}v,$$

where r stands for the charge density in the actual state. It follows from this relation and Eqs. (9) and (11) that

$$\int_{\partial\Omega} J\mathbf{h}\cdot\mathbf{F}^{-\top}\cdot\mathbf{N}\mathrm{d}A = \int_{\Omega} R\mathrm{d}V, \tag{19}$$

where the charge density in the initial state $R = rJ$ is given by

$$R = e(C_{\mathrm{H}^+} - C_{\mathrm{OH}^-} - C_{\mathrm{Cl}^-} - \alpha C_b), \tag{20}$$

and e stands for the charge of the electron. Applying the Stokes formula to Eq. (19) and introducing the nominal electric displacement

$$\mathbf{H} = J\mathbf{F}^{-1}\cdot\mathbf{h} = J\mathbf{h}\cdot\mathbf{F}^{-\top}, \tag{21}$$

we arrive at the equation

$$\nabla_0\cdot\mathbf{H} = R. \tag{22}$$

It follows from Eqs. (8), (18), and (21) that

$$\mathbf{H} = \epsilon J\mathbf{C}^{-1}\cdot\mathbf{E} = \epsilon J\mathbf{E}\cdot\mathbf{C}^{-1}. \tag{23}$$

Combination of Eqs. (15), (20), (22), and (23) results in the Poisson equation

$$\nabla_0\cdot(\epsilon J\mathbf{C}^{-1}\cdot\nabla_0\Phi) = -e(C_{\mathrm{H}^+} - C_{\mathrm{OH}^-} - C_{\mathrm{Cl}^-} - \alpha C_b). \tag{24}$$

For an ideal dielectric that occupies a domain Ω in the initial state and a domain ω in the actual state, the energy of the electric field is given by [29]

$$\int_{\omega}\frac{\mathbf{h}\cdot\mathbf{h}}{2\epsilon}\mathrm{d}v = \int_{\Omega}\frac{1}{2\epsilon J}\mathbf{H}\cdot\mathbf{C}\cdot\mathbf{H}\mathrm{d}V,$$

where Eqs. (8) and (21) are used. It follows from this relation that the free energy density of the electric field formed by mobile ions and bound charges (per unit volume in the initial configuration) reads

$$W_{\mathrm{el}} = \frac{1}{2\epsilon J}\mathbf{H}\cdot\mathbf{C}\cdot\mathbf{H}. \tag{25}$$

For an arbitrary domain Ω, the work of the electric field (per unit time) is determined by [29]

$$\mathcal{U}_{\mathrm{el}} = -\int_{\partial\Omega}\Phi\dot{\mathbf{H}}\cdot\mathbf{N}\mathrm{d}A,$$

where the overdot stands for the derivative with respect to time. Transforming the integral by means of the Stokes formula and

applying Eqs. (15) and (22), we find that

$$\mathcal{U}_{\rm el} = \int_\Omega (\mathbf{E}\cdot\dot{\mathbf{H}} - \Phi\dot{R})dV.$$

It follows from this relation and Eq. (20) that the work of the electric field (per unit volume in the initial configuration and unit time) reads

$$u_{\rm el} = \mathbf{E}\cdot\dot{\mathbf{H}} - e\Phi(\dot{C}_{\rm H^+} - \dot{C}_{\rm OH^-} - \dot{C}_{\rm Cl^-} - \dot{\alpha}C_b). \quad (26)$$

D. Kinetic relations

Denote by $\mathbf{J}$, $\mathbf{J}_{\rm H^+}$, $\mathbf{J}_{\rm Na^+}$, $\mathbf{J}_{\rm OH^-}$, and $\mathbf{J}_{\rm Cl^-}$ the flux vectors for solvent molecules and mobile ions in the initial configuration (numbers of species moving through a unit area per unit time). Their counterparts in the actual configuration read $\mathbf{j}$, $\mathbf{j}_{\rm H^+}$, $\mathbf{j}_{\rm Na^+}$, $\mathbf{j}_{\rm OH^-}$, and $\mathbf{j}_{\rm Cl^-}$. Keeping in mind that $\mathbf{n}\cdot\mathbf{j}da = \mathbf{N}\cdot\mathbf{J}dA$, we find from Eq. (11) that

$$\mathbf{J} = J\mathbf{F}^{-1}\cdot\mathbf{j}, \quad \mathbf{J}_{\rm H^+} = J\mathbf{F}^{-1}\cdot\mathbf{j}_{\rm H^+}, \quad \mathbf{J}_{\rm OH^-} = J\mathbf{F}^{-1}\cdot\mathbf{j}_{\rm OH^-},$$
$$\mathbf{J}_{\rm Cl^-} = J\mathbf{F}^{-1}\cdot\mathbf{j}_{\rm Cl^-}. \quad (27)$$

The flux of solvent in the actual configuration is described by the relation

$$\mathbf{j} = -\frac{Dc}{k_BT}\nabla\mu, \quad (28)$$

where T is the absolute temperature, k_B is Boltzmann's constant, D is the solvent diffusivity, and μ is the chemical potential of water molecules in the gel. It follows from Eqs. (14), (17), (27), and (28) that

$$\mathbf{J} = -\frac{DC}{k_BT}\mathbf{F}^{-1}\cdot\nabla_0\mu\cdot\mathbf{F}^{-1}. \quad (29)$$

Insertion of Eq. (29) into the mass conservation law for solvent,

$$\dot{C} = -\nabla_0\cdot\mathbf{J}, \quad (30)$$

implies that

$$\dot{C} = \nabla_0\cdot\left(\frac{DC}{k_BT}\mathbf{F}^{-1}\cdot\nabla_0\mu\cdot\mathbf{F}^{-1}\right). \quad (31)$$

Denote by $\mu_{\rm H^+}$, $\mu_{\rm OH^-}$, and $\mu_{\rm Cl^-}$ the chemical potentials of mobile ions. Their flux vectors in the initial state are determined by analogy with Eq. (29),

$$\mathbf{J}_{\rm H^+} = -\frac{D_{\rm H^+}C_{\rm H^+}}{k_BT}\mathbf{F}^{-1}\cdot\nabla\mu_{\rm H^+}\cdot\mathbf{F}^{-1},$$
$$\mathbf{J}_{\rm OH^-} = -\frac{D_{\rm OH^-}C_{\rm OH^-}}{k_BT}\mathbf{F}^{-1}\cdot\nabla\mu_{\rm OH^-}\cdot\mathbf{F}^{-1}, \quad (32)$$
$$\mathbf{J}_{\rm Cl^-} = -\frac{D_{\rm Cl^-}C_{\rm Cl^-}}{k_BT}\mathbf{F}^{-1}\cdot\nabla\mu_{\rm Cl^-}\cdot\mathbf{F}^{-1},$$

where $D_{\rm H^+}$, $D_{\rm OH^-}$, and $D_{\rm Cl^-}$ represent the corresponding diffusivities. The mass conservation laws for mobile ions are given by

$$\dot{C}_{\rm H^+} = -\nabla_0\cdot\mathbf{J}_{\rm H^+} + \Gamma_{\rm H^+}, \quad \dot{C}_{\rm OH^-} = -\nabla_0\cdot\mathbf{J}_{\rm OH^-},$$
$$\dot{C}_{\rm Cl^-} = -\nabla_0\cdot\mathbf{J}_{\rm Cl^-}, \quad (33)$$

where

$$\Gamma_{\rm H^+} = \dot{\alpha}C_b \quad (34)$$

is the rate of production of $\rm H^+$ ions caused by dissociation of nonionized functional groups. Insertion of Eqs. (32) and (34) into Eq. (33) implies that

$$\dot{C}_{\rm H^+} = \nabla_0\cdot\left(\frac{D_{\rm H^+}C_{\rm H^+}}{k_BT}\mathbf{F}^{-1}\cdot\nabla_0\mu_{\rm H^+}\cdot\mathbf{F}^{-1}\right) + \dot{\alpha}C_b,$$
$$\dot{C}_{\rm OH^-} = \nabla_0\cdot\left(\frac{D_{\rm OH^-}C_{\rm OH^-}}{k_BT}\mathbf{F}^{-1}\cdot\nabla_0\mu_{\rm OH^-}\cdot\mathbf{F}^{-1}\right), \quad (35)$$
$$\dot{C}_{\rm Cl^-} = \nabla_0\cdot\left(\frac{D_{\rm Cl^-}C_{\rm Cl^-}}{k_BT}\mathbf{F}^{-1}\cdot\nabla_0\mu_{\rm Cl^-}\cdot\mathbf{F}^{-1}\right).$$

For an arbitrary domain Ω with boundary $\partial\Omega$, the work produced by transport of solvent and solutes per unit time reads [29]

$$\mathcal{U}_{\rm dif} = -\int_{\partial\Omega}(\mu\mathbf{J} + \mu_{\rm H^+}\mathbf{J}_{\rm H^+} + \mu_{\rm OH^-}\mathbf{J}_{\rm OH^-} + \mu_{\rm Cl^-}\mathbf{J}_{\rm Cl^-})\cdot\mathbf{N}dA.$$

Transforming the integral by means of the Stokes formula and using (30), (33), and (34), we find that

$$\mathcal{U}_{\rm dif} = -\int_\Omega(\mathbf{J}\cdot\nabla_0\mu + \mathbf{J}_{\rm H^+}\cdot\nabla_0\mu_{\rm H^+} + \mathbf{J}_{\rm OH^-}\cdot\nabla_0\mu_{\rm OH^-}$$
$$+ \mathbf{J}_{\rm Cl^-}\cdot\nabla_0\mu_{\rm Cl^-})dV + \int_\Omega[\mu\dot{C} + \mu_{\rm H^+}(\dot{C}_{\rm H^+} - \dot{\alpha}C_b)$$
$$+ \mu_{\rm OH^-}\dot{C}_{\rm OH^-} + \mu_{\rm Cl^-}\dot{C}_{\rm Cl^-}]dV.$$

It follows from this relation and Eqs. (29) and (32) that the work produced by transport of solvent and solutes (per unit volume in the initial configuration and unit time) is given by

$$u_{\rm dif} = \mu\dot{C} + \mu_{\rm H^+}(\dot{C}_{\rm H^+} - \dot{\alpha}C_b) + \mu_{\rm OH^-}\dot{C}_{\rm OH^-}$$
$$+ \mu_{\rm Cl^-}\dot{C}_{\rm Cl^-} + \bar{u}_{\rm dif}, \quad (36)$$

where

$$\bar{u}_{\rm dif} \geqslant 0. \quad (37)$$

E. Kinematic relations

The reference configuration of the polymer network (in which stresses in chains vanish) is presumed to differ from the initial configuration. Transformation of the initial state into the reference state takes into account evolution of the stress-free state of the network induced by swelling and ionization of functional groups. This transformation is described by the deformation gradient $\mathbf{f}$. For an isotropic polymer network,

$$\mathbf{f} = f^{\frac{1}{3}}\mathbf{I}, \quad (38)$$

where f stands for the coefficient of volume expansion driven by electrostatic repulsion of bound charges, and $\mathbf{I}$ is the unit tensor.

The deformation gradient for elastic deformation $\mathbf{F}_e$ describes the transformation of the reference configuration into the actual configuration. This tensor is connected with the deformation gradient for macrodeformation $\mathbf{F}$ by the multiplicative decomposition formula $\mathbf{F} = \mathbf{F}_e\cdot\mathbf{f}$. Substitution of Eq. (38) into this equation implies that

$$\mathbf{F} = f^{\frac{1}{3}}\mathbf{F}_e. \quad (39)$$

Equation (39) resembles the conventional relation in thermoelasticity, where f describes the evolution of the reference state

induced by changes in temperature. Differentiation of Eq. (39) with respect to time results in

$$\mathbf{D} = \mathbf{D}_e + \frac{\dot{f}}{3f}\mathbf{I}, \tag{40}$$

where

$$\mathbf{L} = \dot{\mathbf{F}} \cdot \mathbf{F}^{-1}, \quad \mathbf{L}_e = \dot{\mathbf{F}}_e \cdot \mathbf{F}_e^{-1} \tag{41}$$

stand for the velocity gradients, and

$$\mathbf{D} = \tfrac{1}{2}(\mathbf{L} + \mathbf{L}^\top), \quad \mathbf{D}_e = \tfrac{1}{2}\left(\mathbf{L}_e + \mathbf{L}_e^\top\right) \tag{42}$$

denote the rate-of-strain tensors.

The Cauchy-Green tensors for elastic deformation are given by

$$\mathbf{B}_e = \mathbf{F}_e \cdot \mathbf{F}_e^\top, \quad \mathbf{C}_e = \mathbf{F}_e^\top \cdot \mathbf{F}_e. \tag{43}$$

The principal invariants J_{e1}, J_{e2}, J_{e3} of these tensors are connected with the principal invariants J_1, J_2, J_3 of the Cauchy-Green tensors for macrodeformation, (8), by the formulas

$$J_1 = f^{\frac{2}{3}} J_{e1}, \quad J_2 = f^{\frac{4}{3}} J_{e2}, \quad J_3 = f^2 J_{e3}. \tag{44}$$

The derivatives of J_{e1}, J_{e2}, J_{e3} with respect to time read

$$\dot{J}_{e1} = 2\mathbf{B}_e : \mathbf{D}_e, \quad \dot{J}_{e2} = 2\left(J_{e2}\mathbf{I} - J_{e3}\mathbf{B}_e^{-1}\right) : \mathbf{D}_e,$$
$$\dot{J}_{e3} = 2J_{e3}\mathbf{I} : \mathbf{D}_e,$$

where the colon stands for convolution of tensors. Insertion of Eq. (40) into these relations implies that

$$\dot{J}_{e1} = 2\mathbf{B}_e : \mathbf{D} - \frac{2\dot{f}}{3f} J_{e1},$$
$$\dot{J}_{e2} = -2\mathbf{B}_e^{-1} : \mathbf{D} J_{e3} + 2\left(\mathbf{I} : \mathbf{D} - \frac{2\dot{f}}{3f}\right) J_{e2}, \tag{45}$$
$$\dot{J}_{e3} = 2\left(\mathbf{I} : \mathbf{D} - \frac{\dot{f}}{f}\right) J_{e3}.$$

F. Free energy density

Denote by Ψ the Helmholtz free energy of a gel per unit volume in the initial configuration. For the three-phase medium, this quantity equals the sum of six components: (i) the energy of solvent and solutes not interacting with each other and with the solid phase Ψ_1, (ii) the energy of the solid phase not interacting with solvent and solutes Ψ_2, (iii) the energy of mixing of the solid phase and water Ψ_3, (iv) the energy of mixing of water and mobile ions Ψ_4, (v) the energy of mixing of charged and noncharged functional groups distributed along polymer chains Ψ_5, and (vi) the energy of the electric field formed by mobile ions and bound charges $W_{\rm el}$,

$$\Psi = \Psi_1 + \Psi_2 + \Psi_3 + \Psi_4 + \Psi_5 + W_{\rm el}. \tag{46}$$

The specific energy density Ψ_1 is given by [26]

$$\Psi_1 = \mu^0 C + \mu^0_{\rm H^+} C_{\rm H^+} + \mu^0_{\rm OH^-} C_{\rm OH^-} + \mu^0_{\rm Cl^-} C_{\rm Cl^-}, \tag{47}$$

where μ^0, $\mu^0_{\rm H^+}$, $\mu^0_{\rm OH^-}$, $\mu^0_{\rm Cl^-}$ denote the chemical potentials of noninteracting water molecules and mobile ions.

The free energy density of the polymer network not interacting with solvent and solutes reads

$$\Psi_2 = W(J_{e1}, J_{e2}, J_{e3}, \alpha, f), \tag{48}$$

where W is the sum of the specific mechanical energy stored in chains and the energy of electrostatic interaction of bound charges. This quantity is treated as a function of the principal invariants of the Cauchy-Green tensor for elastic deformation (in accord with the conventional approach in thermoelasticity), degree of ionization of chains α (the energy of repulsion of ionized functional groups is proportional to this parameter), and coefficient of volume expansion of the network f (the energy of Coulomb forces between bound charges depends on the principal invariants of the Cauchy-Green tensor for macrodeformation, which are expressed in terms of J_{em} and f by Eq. (44)).

With reference to the Flory-Huggins theory [30,31], the specific energy of mixing water molecules with polymer chains reads

$$\Psi_3 = k_B T C \left(\ln\frac{Cv}{1+Cv} + \frac{\chi}{1+Cv}\right), \tag{49}$$

where χ stands for the Flory-Huggins interaction parameter.

The energies of mixing mobile ions with water molecules and mixing ionized and neutral functional groups distributed along chains are determined by the conventional formulas [26]

$$\Psi_4 = k_B T \left[C_{\rm H^+}\left(\ln\frac{C_{\rm H^+}}{C} - 1\right) + C_{\rm OH^-}\left(\ln\frac{C_{\rm OH^-}}{C} - 1\right) + C_{\rm Cl^-}\left(\ln\frac{C_{\rm Cl^-}}{C} - 1\right)\right],$$
$$\Psi_5 = k_B T C_b[\alpha\ln\alpha + (1-\alpha)\ln(1-\alpha)]. \tag{50}$$

G. Free energy imbalance inequality

To develop constitutive equations for a gel under isothermal deformation with finite strains, we apply the free energy imbalance inequality

$$\dot{\Psi} - u_{\rm mech} - u_{\rm el} - u_{\rm dif} - u_{\rm dis} \leqslant 0, \tag{51}$$

where $u_{\rm mech}$, $u_{\rm el}$, $u_{\rm dif}$, and $u_{\rm dis}$ are the works (per unit volume in the initial state and unit time) produced by stresses, electric field, transport of solvent and solutes, and dissociation of functional groups.

The mechanical work is determined by the conventional formula

$$u_{\rm mech} = J\mathbf{T} : \mathbf{D}, \tag{52}$$

where $\mathbf{T}$ is the Cauchy stress tensor. The works performed by the electric field and diffusion of solvent and solutes are given by Eqs. (26) and (36), respectively. The work induced by dissociation of functional groups and formation of ion pairs reads

$$u_{\rm dis} = \dot{\alpha}\Delta\mu C_b, \tag{53}$$

where the constant $\Delta\mu$ stands for the difference in chemical potentials between noncharged and charged functional groups.

Equation (51) is satisfied when functions C and $\mathbf{F}$ are connected by the molecular incompressibility condition, (12).

This condition is accounted for by means of a Lagrange multiplier. We differentiate Eq. (12) with respect to time, use Eq. (A6), and find that

$$\dot{C}v - J\mathbf{I} : \mathbf{D} = 0. \tag{54}$$

Multiplying Eq. (54) by an arbitrary function Π and summing the result with Eq. (51), we obtain

$$\dot{\Psi} + \Pi(\dot{C}v - J\mathbf{I} : \mathbf{D}) - u_{\rm mech} - u_{\rm el} - u_{\rm dif} - u_{\rm dis} \leqslant 0. \tag{55}$$

Differentiating Eq. (46) with respect to time and using Eqs. (25) and (47)–(50), we find that

$$\begin{aligned}\dot{\Psi} = {} & 2(\mathbf{K}_{\rm mech}+\mathbf{K}_{\rm el}) : \mathbf{D}+\mathbf{E}\cdot\dot{\mathbf{H}}+\left[W_{,\alpha}\dot{\alpha} - \left(\frac{2K}{3f} - W_{,f}\right)\dot{f}\right] \\ & + \Theta_C\dot{C} + \Theta_{\rm H^+}\dot{C}_{\rm H^+} + \Theta_{\rm OH^-}\dot{C}_{\rm OH^-} + \Theta_{\rm Cl^-}\dot{C}_{\rm Cl^-} \\ & + \Theta_\alpha\dot{\alpha}C_b,\end{aligned} \tag{56}$$

where the coefficients are determined by Eqs. (A3), (A9), and (A10). Substitution of Eqs. (26), (36), (52), (53), and (56) into Eq. (55) implies that

$$\begin{aligned}& [2(\mathbf{K}_{\rm mech} + \mathbf{K}_{\rm pol}) - J(\mathbf{T} + \Pi\mathbf{I})] : \mathbf{D} \\ & + \left[W_{,\alpha}\dot{\alpha} - \left(\frac{2K}{3f} - W_{,f}\right)\dot{f}\right] \\ & + (\Theta_C + \Pi v - \mu)\dot{C} + (\Theta_{\rm H^+} + e\Phi - \mu_{\rm H^+})\dot{C}_{\rm H^+} \\ & + (\Theta_{\rm OH^-} - e\Phi - \mu_{\rm OH^-})\dot{C}_{\rm OH^-} + (\Theta_{\rm Cl^-} - e\Phi - \mu_{\rm Cl^-})\dot{C}_{\rm Cl^-} \\ & + (\Theta_\alpha + \mu_{\rm H^+} - e\Phi - \Delta\mu)\dot{\alpha}C_b - \bar{u}_{\rm dif} \leqslant 0.\end{aligned} \tag{57}$$

Using Eq. (37) and keeping in mind that $\mathbf{D}$, C, $C_{\rm H^+}$, $C_{\rm OH^-}$, $C_{\rm Cl^-}$, and α are arbitrary functions, we conclude that Eq. (57) is fulfilled, provided that (i) the Cauchy stress tensor reads

$$\mathbf{T} = -\Pi\,\mathbf{I} + \frac{2}{J}(\mathbf{K}_{\rm mech} + \mathbf{K}_{\rm el}); \tag{58}$$

(ii) the chemical potentials of water molecules and mobile ions are given by

$$\begin{aligned}\mu = \Theta_C + \Pi v, \quad \mu_{\rm H^+} = \Theta_{\rm H^+} + e\Phi, \\ \mu_{\rm OH^-} = \Theta_{\rm OH^-} - e\Phi, \\ \mu_{\rm Cl^-} = \Theta_{\rm Cl^-} - e\Phi;\end{aligned} \tag{59}$$

(iii) the degree of ionization obeys the equation

$$\Theta_\alpha + \mu_{\rm H^+} - e\Phi - \Delta\mu = 0; \tag{60}$$

and (iv) volume expansion for the polymer network is governed by the equation

$$\left(\frac{2K}{3f} - W_{,f}\right)\dot{f} = W_{,\alpha}\dot{\alpha}. \tag{61}$$

In the derivation of the governing equations, the term $W_{,\alpha}\dot{\alpha}$ is included in Eq. (61) based on the assumption that the energy of electrostatic repulsion of bound changes is too weak to affect the ionization process but is sufficiently strong to change the reference state of the polymer network.

To transform Eq. (58), we substitute Eqs. (12), (A3), and (A9) in this relation and find that

$$\begin{aligned}\mathbf{T} = -\Pi\,\mathbf{I} + \frac{2}{1+Cv}\big[W_{,1}\mathbf{B}_e - J_{e3}W_{,2}\mathbf{B}_e^{-1} \\ + (J_{e2}W_{,2} + J_{e3}W_{,3})\mathbf{I}\big] + \mathbf{T}_M,\end{aligned} \tag{62}$$

where

$$\mathbf{T}_M = \frac{1}{\epsilon}\left[(\mathbf{h}\otimes\mathbf{h}) - \frac{1}{2}(\mathbf{h}\cdot\mathbf{h})\mathbf{I}\right] \tag{63}$$

represents the Maxwell stress [32].

Insertion of Eq. (A10) into Eqs. (59) yields

$$\begin{aligned}\mu = {} & \mu^0 + k_BT\left[\ln\frac{Cv}{1+Cv} + \frac{1}{1+Cv} + \frac{\chi}{(1+Cv)^2} + \frac{\Pi v}{k_BT}\right. \\ & \left. - \frac{C_{\rm H^+} + C_{\rm OH^-} + C_{\rm Cl^-}}{C}\right], \\ \mu_{\rm H^+} = {} & \mu^0_{\rm H^+} + k_BT\ln\frac{C_{\rm H^+}}{C} + e\Phi, \\ \mu_{\rm OH^-} = {} & \mu^0_{\rm OH^-} + k_BT\ln\frac{C_{\rm OH^-}}{C} - e\Phi, \\ \mu_{\rm Cl^-} = {} & \mu^0_{\rm Cl^-} + k_BT\ln\frac{C_{\rm Cl^-}}{C} - e\Phi.\end{aligned} \tag{64}$$

It is worth noting that formulas (64) involve components proportional to the electrostatic potential Φ, which means that the model does not require the chemical and electrochemical potentials of mobile ions to be distinguished [due to the accounting for the energy of the electric field in Eq. (51)].

It follows from Eqs. (60), (64), and (A10) that

$$\ln\frac{1-\alpha}{\alpha} = \ln\frac{C_{\rm H^+}}{C} - \ln {\rm K}'_{\rm a}, \tag{65}$$

where the acid dissociation constant reads

$${\rm K}'_{\rm a} = \exp\left(\frac{\Delta\mu - \mu^0_{\rm H^+}}{k_BT}\right). \tag{66}$$

Resolving Eq. (65) with respect to α, we arrive at the Henderson-Hasselbach equation,

$$\alpha = {\rm K}'_{\rm a}\left({\rm K}'_{\rm a} + \frac{C_{\rm H^+}}{C}\right)^{-1}. \tag{67}$$

It should be mentioned that Eq. (67) does not contain a multiplier proportional to the degree of swelling introduced in phenomenological extensions of the Henderson-Hasselbach equation [27].

Constitutive equations for a *p*H-sensitive gel involve (i) stress-strain relations (62) and (63), (ii) Eqs. (64) for chemical potentials of solvent and solutes, (iii) Eqs. (67) for degree of ionization of chains, and (iv) Eq. (61) for coefficient of inflation of the polymer network. These relations are accompanied by (i) the equilibrium equation for the Cauchy stress tensor, (ii) reaction-diffusion Eqs. (31) and (35) for solvent and solutes, and (iii) Eq. (24) for the electrostatic potential together with the appropriate initial and boundary conditions.

H. Simplification of the model

Although the governing equations describe basic electromechanical processes in a *p*H-responsive gel under swelling, these relations appear to be overly complicated for practical applications. To simplify the model, we disregard the Maxwell stress, (63), compared with the mechanical

stress

$$\mathbf{T} = -\Pi\,\mathbf{I} + \frac{2}{1+Cv}\big[W_{,1}\mathbf{B}_e - J_{e3}W_{,2}\mathbf{B}_e^{-1} + (J_{e2}W_{,2} + J_{e3}W_{,3})\mathbf{I}\big]. \tag{68}$$

To assess this assumption, we set the characteristic potential drop at the interface between a sample and the bath at 1 mV, the characteristic length of the double layer at the boundary at 0.7 nm, and the relative permittivity $\epsilon_r = 80$, use $\epsilon_0 = 8.85 \times 10^{-12}$ F/m, and conclude that the Maxwell stress does not exceed 10^3 Pa. Setting the characteristic degree of swelling at 30 and the characteristic elastic modulus of a gel at 10^5 Pa, we estimate the characteristic mechanical stress as 3×10^5 Pa, which greatly exceeds the Maxwell stress under equilibrium water uptake.

To further simplify the constitutive equations, we introduce the principle of electromechanical equivalence, which presumes the existence of an equivalent noncharged polymer network with coefficient of volume expansion $f_{\rm eq}(\alpha)$ and elastic energy $W_{\rm eq}(J_{e1}, J_{e2}, J_{e3})$ such that the Cauchy stress in the real (partially ionized) network $\mathbf{T}$ coincides with the Cauchy stress in the equivalent network

$$\mathbf{T}_{\rm eq} = -\Pi\,\mathbf{I} + \frac{2}{1+Cv}\big[W_{{\rm eq},1}\mathbf{B}_e - J_{e3}W_{{\rm eq},2}\mathbf{B}_e^{-1} + (J_{e2}W_{{\rm eq},2} + J_{e3}W_{{\rm eq},3})\mathbf{I}\big].$$

This approach allows (i) differential Eq. (61) to be excluded by replacing it with a phenomenological equation for the function $f_{\rm eq}(\alpha)$ and (ii) conventional formulas to be employed for the elastic energy $W_{\rm eq}$ instead of the complicated expression (48), which depends on five arguments. With reference to this concept, we calculate the Cauchy stress tensor by means of Eq. (68), with W depending on the principal invariants J_{e1}, J_{e2}, and J_{e3} only.

Finally, (i) the neo-Hookean formula is adopted for the strain energy density of the equivalent network,

$$W = \tfrac{1}{2}G[(J_{e1} - 3) - \ln J_{e3}], \tag{69}$$

where G stands for the shear modulus, and (ii) the coefficient of volume expansion of the equivalent network f is presumed to increase linearly with the concentration of bound charges,

$$f = 1 + q_0 + q_1 C_b \alpha, \tag{70}$$

where q_0 stands for the degree of swelling of an as-prepared gel, and q_1 is a material constant. The physical meaning of Eq. (69) was discussed in [33], where this formula was "rederived" within the concept of entropic elasticity. More sophisticated expressions for W were developed in [34] and [35].

III. EQUILIBRIUM SWELLING UNDER HOMOGENEOUS DEFORMATIONS

To examine the ability of the model to describe observations, the governing equations are applied to fit experimental swelling diagrams on polyelectrolyte gels. With reference to [36], it is assumed that in a specimen fully swollen under homogeneous deformation, (i) concentrations of solvent and solutes are independent of spatial coordinates, and (ii) the electrostatic potential is independent of spatial coordinates but adopts different values, Φ and $\bar\Phi$, in the gel and in the bath. The difference between these quantities characterizes the strength of an electric double layer on the boundary of a sample (whose thickness is disregarded compared with the characteristic size of the specimen).

A. Donnan equilibrium

Under equilibrium conditions, chemical potentials of solvent and solutes in a gel and in the bath coincide,

$$\mu = \bar\mu, \quad \mu_{\rm H^+} = \bar\mu_{\rm H^+}, \quad \mu_{\rm OH^-} = \bar\mu_{\rm OH^-}, \quad \mu_{\rm Cl^-} = \bar\mu_{\rm Cl^-}, \tag{71}$$

where the overbar denotes parameters of the bath. Insertion of Eq. (64) into Eq. (71) implies that

$$\begin{aligned} \ln\frac{C_{\rm H^+}}{C} &= \ln\frac{\bar c_{\rm H^+}}{\bar c} - \frac{e}{k_BT}(\Phi - \bar\Phi),\\ \ln\frac{C_{\rm OH^-}}{C} &= \ln\frac{\bar c_{\rm OH^-}}{\bar c} + \frac{e}{k_BT}(\Phi - \bar\Phi),\\ \ln\frac{C_{\rm Cl^-}}{C} &= \ln\frac{\bar c_{\rm Cl^-}}{\bar c} + \frac{e}{k_BT}(\Phi - \bar\Phi), \end{aligned} \tag{72}$$

where the concentrations of water molecules and mobile ions in the bath in the initial configuration are replaced with their concentrations in the actual configuration. It follows from Eq. (72) that

$$\frac{C_{\rm H^+}}{C}\frac{C_{\rm OH^-} + C_{\rm Cl^-}}{C} = \frac{\bar c_{\rm H^+}}{\bar c}\frac{\bar c_{\rm OH^-} + \bar c_{\rm Cl^-}}{\bar c}. \tag{73}$$

The electroneutrality conditions for the gel and for the bath read

$$C_{\rm OH^-} + C_{\rm Cl^-} = C_{\rm H^+} - \alpha C_b, \quad \bar c_{\rm OH^-} + \bar c_{\rm Cl^-} = \bar c_{\rm H^+}. \tag{74}$$

Substituting expressions (74) into Eq. (73) and using Eqs. (2) and (7), we arrive at the equation

$$X\left(X - \alpha\frac{C_b}{C}\right) = \frac{1}{\kappa^2}10^{-2p\rm H}, \tag{75}$$

where

$$X = \frac{C_{\rm H^+}}{C} \tag{76}$$

denotes the concentration of counterions in a gel.

The chemical potential of water molecules in the gel is determined by Eq. (64). Their chemical potential in the bath is given by the same equation, where the first four terms in square brackets (which describe interaction between the polymer network and the solvent) are disregarded, $\bar\mu = \mu^0 - k_BT(\bar c_{\rm H^+} + \bar c_{\rm OH^-} + \bar c_{\rm Cl^-})/\bar c$. Substitution of these expressions into Eq. (71) implies that

$$\ln\frac{Cv}{1+Cv} + \frac{1}{1+Cv} + \frac{\chi}{(1+Cv)^2} + \frac{v}{k_BT}(\Pi - \Pi_{\rm ion}) = 0, \tag{77}$$

where the ionic pressure $\Pi_{\rm ion}$ is given by

$$\Pi_{\rm ion} = \frac{k_BT}{v}\left(\frac{C_{\rm H^+} + C_{\rm OH^-} + C_{\rm Cl^-}}{C} - \frac{\bar c_{\rm H^+} + \bar c_{\rm OH^-} + \bar c_{\rm Cl^-}}{\bar c}\right). \tag{78}$$

Applying Eqs. (12)–(14), we present Eq. (78) in the form $\Pi_{\rm ion} = \Pi^*_{\rm ion} + \Delta\Pi_{\rm ion}$, where

$$\Pi^*_{\rm ion} = k_B T[(c_{\rm H^+} + c_{\rm OH^-} + c_{\rm Cl^-}) - (\bar{c}_{\rm H^+} + \bar{c}_{\rm OH^-} + \bar{c}_{\rm Cl^-})]$$

is the van't Hoff ionic pressure, and $\Delta\Pi_{\rm ion} = k_B T(c_{\rm H^+} + c_{\rm OH^-} + c_{\rm Cl^-})/J$ accounts for deviations from the van't Hoff law. Keeping in mind that $\Delta\Pi_{\rm ion}$ vanishes at $J \gg 1$, we conclude that the van't Hoff law follows from the model for highly swollen gels.

It follows from Eqs. (2), (7), (74), and (76) that

$$\frac{C_{\rm H^+} + C_{\rm OH^-} + C_{\rm Cl^-}}{C} = 2X - \frac{\alpha C_b}{C},$$
$$\frac{\bar{c}_{\rm H^+} + \bar{c}_{\rm OH^-} + \bar{c}_{\rm Cl^-}}{\bar{c}} = \frac{2}{\kappa}10^{-p\rm H}.$$

Insertion of these expressions into Eq. (78) yields

$$\Pi_{\rm ion} = \frac{k_B T}{v}\left[2\left(X - \frac{1}{\kappa}10^{-p\rm H}\right) - \frac{\alpha C_b}{C}\right]. \tag{79}$$

Equation (75) implies that

$$\left(X - \frac{1}{\kappa}10^{-p\rm H}\right) = \frac{\alpha C_b}{C} X\left(X + \frac{1}{\kappa}10^{-p\rm H}\right)^{-1}.$$

Substitution of this expression into Eq. (79) results in the formula

$$\Pi_{\rm ion} = \frac{k_B T X}{v}\left(\frac{\alpha C_b}{C}\right)^2\left(X + \frac{1}{\kappa}10^{-p\rm H}\right)^{-2}, \tag{80}$$

which implies that $\Pi_{\rm ion}$ is proportional to the squared degree of ionization α, in accord with [37]. Calculating the ratio $\alpha C_b/C$ from Eq. (75) and inserting the result into Eq. (80), we express the ionic pressure in terms of the concentration of counterions X in a gel and pH of the bath,

$$\Pi_{\rm ion} = \frac{k_B T}{Xv}\left(X - \frac{1}{\kappa}10^{-p\rm H}\right)^{-2}. \tag{81}$$

Combining Eqs. (67), (75), (77), and (81) and introducing the notation

$$Q = Cv, \quad Q_b = C_b v, \tag{82}$$

we present the governing equation in the form convenient for simulation,

$$X^2 - \frac{\alpha Q_b}{Q}X = \frac{1}{\kappa^2}10^{-2p\rm H}, \quad \alpha = \frac{\rm K'_a}{\rm K'_a + X}, \tag{83}$$

$$\ln\frac{Q}{1+Q} + \frac{1}{1+Q} + \frac{\chi}{(1+Q)^2} + \frac{\Pi v}{k_B T} - \frac{1}{X}\left(X - \frac{1}{\kappa}10^{-p\rm H}\right)^{-2} = 0. \tag{84}$$

B. Unconstrained swelling

When a dry gel specimen is immersed in a bath and is allowed to swell without constraints, the deformation gradient for macrodeformation reads

$$\mathbf{F} = (1 + Cv)^{\frac{1}{3}}\mathbf{I}. \tag{85}$$

Substitution of Eqs. (70) and (85) into Eq. (39) yields

$$\mathbf{F}_{\rm e} = \left(\frac{1+Cv}{1+q_0+q_1C_b\alpha}\right)^{\frac{1}{3}}\mathbf{I}. \tag{86}$$

It follows from Eqs. (68) and (69) that

$$\mathbf{T} = -\Pi\,\mathbf{I} + \frac{G}{1+Cv}(\mathbf{B}_e - \mathbf{I}). \tag{87}$$

Substitution of Eqs. (12), (43), and (86) into Eq. (87) implies that

$$\mathbf{T} = T\mathbf{I}, \quad T = -\Pi + \frac{G}{1+Cv}\left[\left(\frac{1+Cv}{1+q_0+q_1C_b\alpha}\right)^{\frac{2}{3}} - 1\right].$$

Keeping in mind that $\mathbf{T} = \mathbf{0}$ for a specimen with a traction-free surface, we find that

$$\Pi = \frac{G}{1+Cv}\left[\left(\frac{1+Cv}{1+q_0+q_1C_b\alpha}\right)^{\frac{2}{3}} - 1\right]. \tag{88}$$

It is convenient to present Eq. (88) in the form $\Pi = \Pi^* - \Pi_{\rm rep}$, where

$$\Pi^* = \frac{G}{1+Cv}\left[\left(\frac{1+Cv}{1+q_0}\right)^{\frac{2}{3}} - 1\right]$$

stands for the osmotic pressure in the nonionized gel, and

$$\Pi_{\rm rep} = \frac{G}{1+Q}\left[\left(\frac{1+Cv}{1+q_0}\right)^{\frac{2}{3}} - \left(\frac{1+Cv}{1+q_0+q_1C_b\alpha}\right)^{\frac{2}{3}}\right] \tag{89}$$

describes the pressure induced by the repulsive interaction between bound charges.

Inserting Eq. (88) into Eq. (84), using Eq. (82), and setting

$$g = \frac{Gv}{k_B T}, \quad \bar{q} = \frac{q_1}{v}, \tag{90}$$

we obtain

$$\ln\frac{Q}{1+Q} + \frac{1}{1+Q} + \frac{\chi}{(1+Q)^2} + \frac{g}{1+Q}\left[\left(\frac{1+Q}{1+q_0+\bar{q}Q_b\alpha}\right)^{\frac{2}{3}} - 1\right] - \frac{1}{X}\left(X - \frac{1}{\kappa}10^{-p\rm H}\right)^{-2} = 0. \tag{91}$$

For each pH, Eqs. (83) and (91) determine the degree of swelling Q, degree of ionization of chains α, and concentration of hydroxide ions X. These relations involve six material constants: (i) g is the dimensionless elastic modulus, (ii) Q_b denotes the volume fraction of functional groups in the initial state, (iii) $\rm K_a = \kappa K'_a$ stands for the dissociation constant of these groups, (iv) χ is the Flory-Huggins parameter, and (v, vi) q_0 and $\bar{q}$ describe the evolution of the stress-free state driven by ionization of chains.

C. Fitting of observations

To demonstrate that Eqs. (83) and (91) correctly describe equilibrium swelling diagrams on polyelectrolyte gels, these relations are solved numerically by the Newton-Raphson

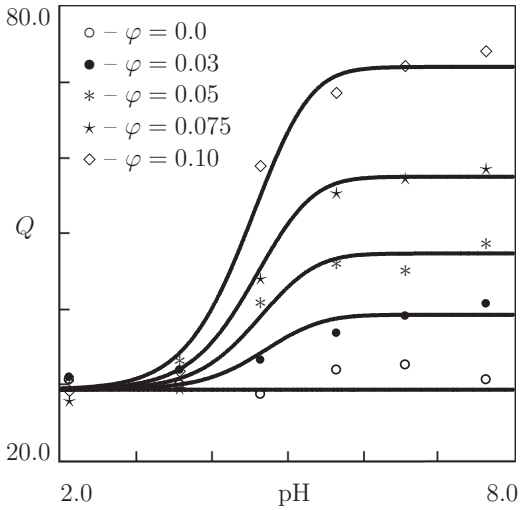

FIG. 1. Degree of swelling Q versus pH. Symbols: experimental data on DMA-IAc gels with various molar fractions of IAc φ [38]. Solid lines: results of simulation.

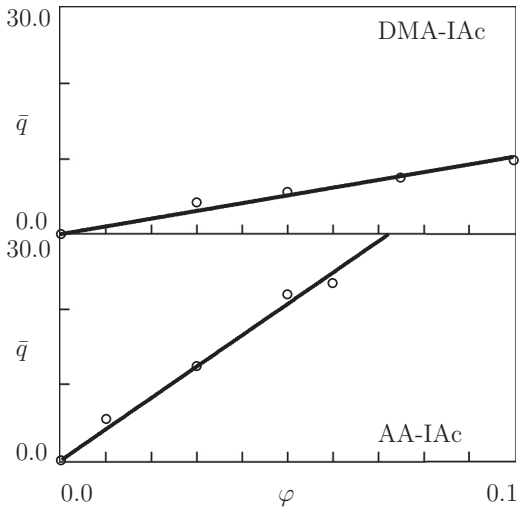

FIG. 2. Coefficient $\bar{q}$ versus molar fraction of IAc φ. Circles: treatment of observations. Solid lines: approximation of the data by Eq. (92).

algorithm, and results of simulation are compared with observations. We begin with the analysis of experimental data on poly(N,N-dimethylacrylamide-itaconic acid) (DMA-IAc) hydrogels [38]. Specimens were prepared by free-radical polymerization of monomers in water using N,N'-methylenebisacrylamide (BAAm) as a cross-linker, ammonium persulfate (APS) as an initiator, and N,N,N',N'-tetramethylethylenediamine (TEMED) as an accelerator. After polymerization of pregel solutions with a monomer concentration of 6.0 wt% and molar fractions of IA φ ranging from 0 to 0.1, samples were immersed in a water bath at room temperature, and their equilibrium degree of swelling was measured at a pH in the interval from 2 to 8. Experimental swelling diagrams on hydrogels with $\varphi = 0, 0.03, 0.05, 0.075$, and 0.10 are depicted in Fig. 1. This figure shows that (i) given φ, the degree of swelling Q increases with pH and reaches its ultimate value when the pH exceeds 7, and (ii) for a fixed pH, Q remains independent of φ at low pH and increases with the concentration of IAc at high pH.

To reduce the number of parameters to be determined by matching observations, we set $\chi = 0.4$ (water is treated as a poor solvent), $q_0 = 0$ (the reference state of noncharged chains coincides with the initial state), and suppose that the volume occupied by functional groups of IAc in the initial state equals $Q_b^0 = 10^{-4}$ of the entire volume occupied by this polymer (which means that $Q_b = Q_b^0\varphi$). Dimensionless elastic modulus $g = 4.2 \times 10^{-4}$ is determined by matching the observations at low pH. According to Eq. (90), where we set $k_B = 1.38 \times 10^{-23}$ kg $\cdot$ m^2/(s$^2 \cdot$ K), $T = 296$K, $v = 2.99 \times 10^{-29}$ m^3, this value corresponds to the shear modulus $G = 5.7 \times 10^4$ Pa, which is typical for polyelectrolyte gels. Coefficient $p\mathrm{K_a} = 4.9$ is found by fitting the swelling curve for the gel with the highest content of IAc and used without changes to approximate observations on the other samples. Keeping in mind that the process of dissociation of IAc involves two steps, our finding is in agreement with the constants $p\mathrm{K_{a1}} = 3.6$ and $p\mathrm{K_{a2}} = 5.5$ determined for dilute solutions of IAc [39]. The only adjustable parameter $\bar{q}$ is calculated from the best-fit condition for each swelling diagram separately.

The effect of φ on $\bar{q}$ is illustrated in Fig. 2, where the data are approximated by the linear equation

$$\bar{q} = \bar{q}_1\varphi, \tag{92}$$

with $\bar{q}_1$ found by the least-squares technique. Equations (70) and (92) express the fact that elongation of chains induced by electrostatic repulsion is proportional to the number of charged groups.

Evolution of the degree of ionization α with pH and φ is reported in Fig. 3. According to this figure, (i) α grows with pH for a given φ and reaches its ultimate value at a pH exceeding 6, whereas (ii) the maximum value of α decreases slightly with φ.

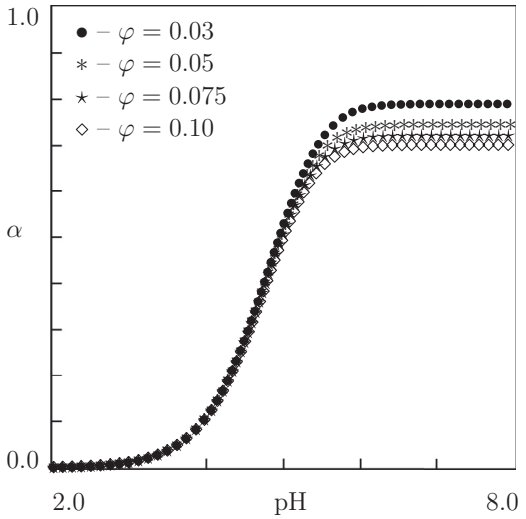

FIG. 3. Degree of ionization α versus pH. Symbols: results of simulation for DMA-IAc gels with various molar fractions of IAc φ.

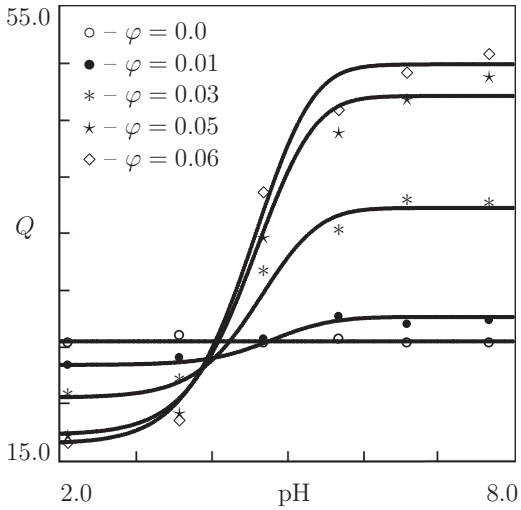

FIG. 4. Degree of swelling Q versus pH. Symbols: experimental data on AA-IAc gels with various molar fractions of IAc φ [38]. Solid lines: results of simulation.

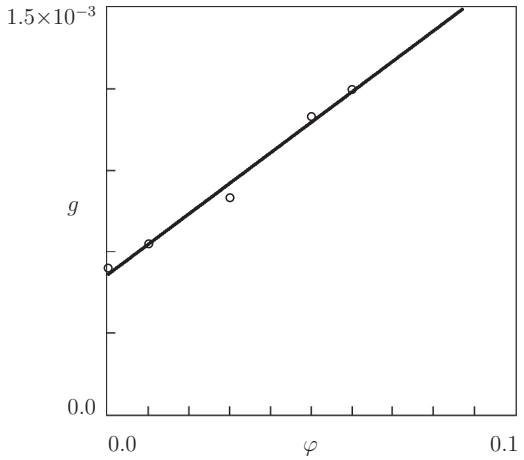

FIG. 5. Coefficient g versus molar fraction of IAc φ. Circles: treatment of observations. Solid line: approximation of the data by Eq. (93).

We proceed with the study of experimental data on poly(acrylamide-itaconic acid; AA-IAc) gels prepared by the same procedure [38]. Experimental swelling diagrams on AA-IAc gels with $\varphi = 0$, 0.01, 0.03, 0.05, and 0.06 are depicted in Fig. 4 together with the results of simulation. Fitting is conducted with the constants χ, q_0, $p\mathrm{K_a}$, and Q_b^0 determined for DMA-IAc gels. As observations reveal a strong dependence of elastic modulus on φ at low pH, each diagram in this figure is approximated by means of two parameters, g and $\bar{q}$.

Changes in $\bar{q}$ with φ are reported in Fig. 2, where the data are approximated by Eq. (92). It is worth noting that the $\bar{q}_1$ of AA-IAc gels exceeds that of DMA-IAc gels by a factor of 4, which means that evolution of the reference state of polymer chains formed by neutral and polyelectrolyte segments depends on the concentration of charged groups and stiffness on neutral segments.

The effect of φ on the dimensionless modulus g is illustrated in Fig. 5. The data are approximated by the linear equation

$$g = g_0 + g_1\varphi, \tag{93}$$

where g_0 and g_1 are found by the least-squares method. According to this figure, g grows linearly with φ, in accord with the rule of mixture for composite media.

Changes in the degree of ionization α with pH and φ are reported in Fig. 6. Comparison of Figs. 3 and 6 shows that α is weakly affected by the chemical structure of the neutral component in copolymer gels (replacement of DMA with AA results in a slight increase in the ultimate value of α only).

Figures 1 and 3 characterize the influence of pH on the degree of swelling of copolymer gels with low concentrations of polyelectrolyte segments. To examine the response of copolymer gels with low concentrations of neutral segments, we analyze observations on poly(vinyl alcohol-aspartic acid; PVA-AsAc) interpenetrating network hydrogels [40]. Specimens were manufactured by the freezing-thawing technique. In the first step, a covalently cross-linked AsAc gel was prepared by reaction polymerization of polysuccinimide in a mixture of N-dimethylformamide (DMF) and water using 1,6-hexanediamine as a cross-linker. In the next step, the dried AsAc powder was added to an aqueous solution of PVA and subjected to six freeze-thaw cycles in which PVA chains were cross-linked by nanocrystallites.

Equilibrium swelling diagrams on gels with mass fractions of AsAc φ ranging from 0.9 to 1.0 are depicted in Fig. 7. Experiments were conducted at a temperature of 37 °C, with the pH of the water bath varied between 1 and 6. In the approximation procedure, we set $\chi = 0.4$, $q_0 = 0$, $Q_b^0 = 10^{-4}$ (the same parameters as in Figs. 1 and 3), determine $g = 0.01$ by matching the data at low pH, and calculate $p\mathrm{K_a} = 2.8$ by fitting observation on a neat AsAc gel. The only adjustable parameter $\bar{q}$ is found from the best-fit condition for each set of data separately. The best-fit value of $p\mathrm{K_a}$ is in accord with the dissociation constants $p\mathrm{K_{a1}} = 2.0$ and $p\mathrm{K_{a2}} = 3.9$ for AsAc [40].

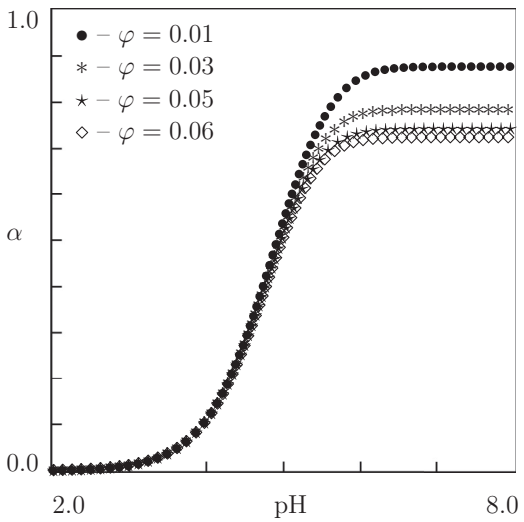

FIG. 6. Degree of ionization α versus pH. Symbols: results of simulation for AA-IAc gels with various molar fractions of IAc φ.

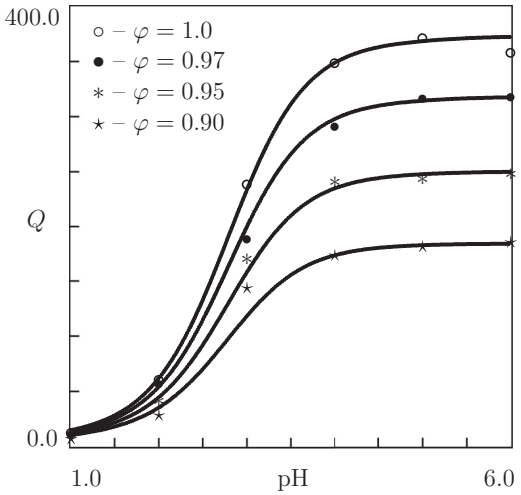

FIG. 7. Degree of swelling Q versus pH. Symbols: experimental data on PVA-AsAc gels with various mass fractions of AsAc φ [40]. Solid lines: results of simulation.

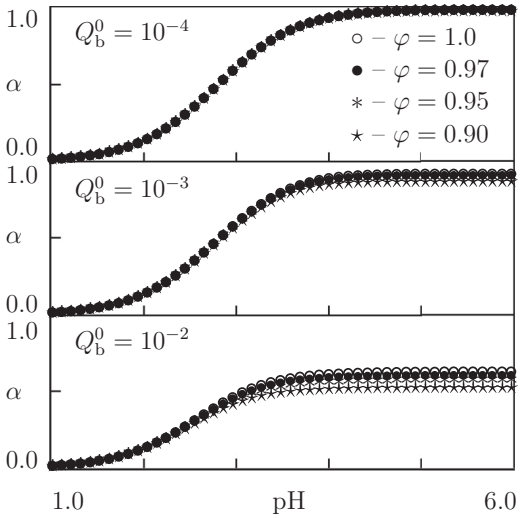

FIG. 9. Degree of ionization α versus pH. Symbols: results of simulation for PVA-AsAc gels with various φ and Q_b^0.

To assess the influence of the volume fraction of functional groups on material constants, the fitting procedure is repeated with $Q_b^0 = 10^{-3}$ and $Q_b^0 = 10^{-2}$. The growth of Q_b^0 by two orders of magnitude does not affect the quality of matching observations (as the results of simulation for various Q_b^0 coincide, the corresponding figures are omitted) but induces an increase in the elastic modulus g (from 0.01 to 0.025) and a pronounced decay in $\bar{q}$.

The effect of φ on $\bar{q}$ is illustrated in Fig. 8, where the data are approximated by the linear equation

$$\bar{q} = \bar{q}_0 + \bar{q}_1\varphi, \tag{94}$$

with coefficients $\bar{q}_0$ and $\bar{q}_1$ determined by the least-squares technique.

The evolution of the degree of ionization of chains with φ and Q_b^0 is reported in Fig. 9, where α is plotted versus pH. This figure reveals that α is affected by our choice of Q_b^0. When Q_b^0 is relatively small, all functional groups become charged at high pH, and the degree of ionization is independent of the mass fraction of polyelectrolyte segments. With an increase in Q_b^0, the fraction of charged groups is reduced (for gels swollen in water with $p\mathrm{H} = 6$, α decreases from 1.0 at $Q_b^0 = 10^{-4}$ to 0.63 at $Q_b^0 = 10^{-2}$ when $\varphi = 1.0$ and to 0.52 when $\varphi = 0.9$). This implies that Q_b^0 can be determined independently of swelling tests by measuring the degree of ionization of chains under basic conditions.

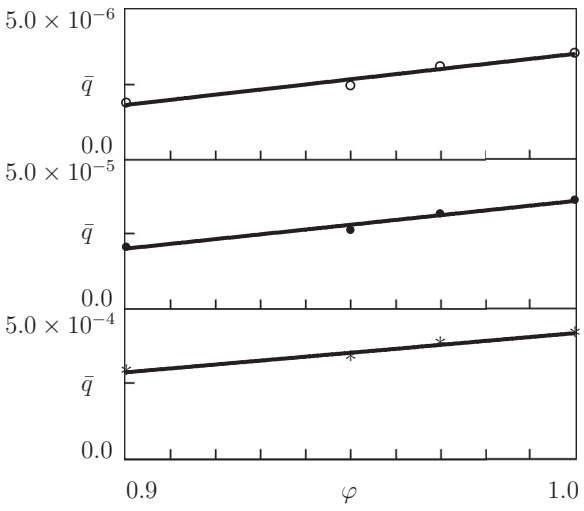

FIG. 8. Coefficient $\bar{q}$ versus mass fraction φ of AsAc. Symbols: treatment of observations on PVA-AsAc gels with $Q_b = 10^{-4}$, 10^{-3}, 10^{-2}. Solid lines: approximation of the data by Eq. (94).

To establish correlations between ionic pressure and repulsive forces between bound charges, simulation of the governing equations is conducted with the material constants determined for AsAc ($\varphi = 1.0$). The dimensionless ionic pressure $\tilde{\Pi}_{\mathrm{ion}} = \Pi_{\mathrm{ion}} v/(k_B T)$ and dimensionless pressure induced by electrostatic interaction of ionized groups $\tilde{\Pi}_{\mathrm{rep}} = \Pi_{\mathrm{rep}} v/(k_B T)$ are determined from Eqs. (81) and (89) and are plotted versus pH in Fig. 10. This figure demonstrates that for all Q_b^0 under consideration, $\tilde{\Pi}_{\mathrm{rep}}$ exceeds $\tilde{\Pi}_{\mathrm{ion}}$ by several orders of magnitude.

To confirm this conclusion, we fit observations on poly(acrylic acid) (AAc) gels [41]. An advantage of these data is that $p\mathrm{K_a} = 4.75$ for AAc is known, which allows the number of adjustable parameters to be reduced. Specimens were prepared by free radical polymerization of AAc monomers dissolved in water using BAAm as a cross-linker (0.1 mol%) and potassium persulfate (KPS) as an initiator.

To approximate observations in Fig. 11, we set $\chi = 0.4$, $q_0 = 0$, determine $g = 0.04$ by matching observations at low pH, and find $Q_b = 5.0 \times 10^{-6}$, $\bar{q} = 5.0 \times 10^6$ from the best-fit condition for the swelling diagram. To demonstrate that these parameters ensure a reasonable degree of ionization of functional groups, α is plotted as a function of pH in Fig. 11. Results of simulation for dimensionless pressures $\tilde{\Pi}_{\mathrm{rep}}$ and $\tilde{\Pi}_{\mathrm{ion}}$ are reported in Fig. 12. According to this figure, $\tilde{\Pi}_{\mathrm{rep}}$ exceeds $\tilde{\Pi}_{\mathrm{ion}}$ by three orders of magnitude at all pH values.

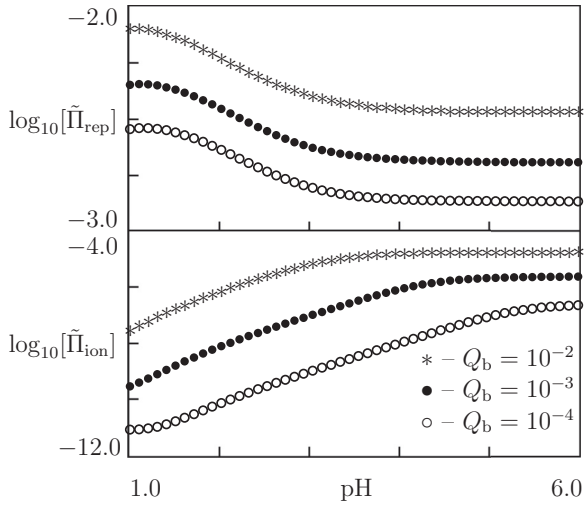

FIG. 10. Pressure driven by repulsion of charges $\tilde{\Pi}_{\rm rep}$ and ionic pressure $\tilde{\Pi}_{\rm ion}$ versus pH. Symbols: results of simulation for AsAc gels with various Q_b^0.

D. Constrained swelling

We study water uptake by a dry cylindrical specimen immersed in a water bath and allowed to swell in the radial direction while the positions of its ends are fixed. The deformation gradient for macrodeformation reads

$$\mathbf{F} = \mathbf{e}_1 \otimes \mathbf{e}_1 + \lambda(\mathbf{e}_2 \otimes \mathbf{e}_2 + \mathbf{e}_3 \otimes \mathbf{e}_3), \tag{95}$$

where $\mathbf{e}_m$ are unit vectors of a Cartesian frame ($\mathbf{e}_1$ is directed along the axis of the cylinder). The coefficient of lateral expansion under swelling λ is determined from Eqs. (12) and (95):

$$\lambda = (1 + Cv)^{\frac{1}{2}}. \tag{96}$$

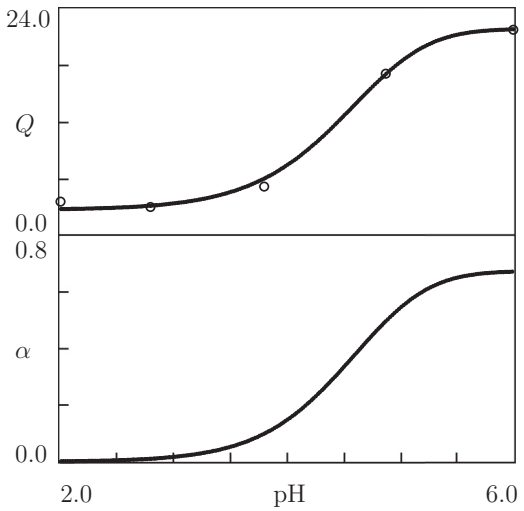

FIG. 11. Degree of swelling Q and degree of ionization α versus pH. Circles: experimental data on AAc gel [41]. Solid lines: results of simulation.

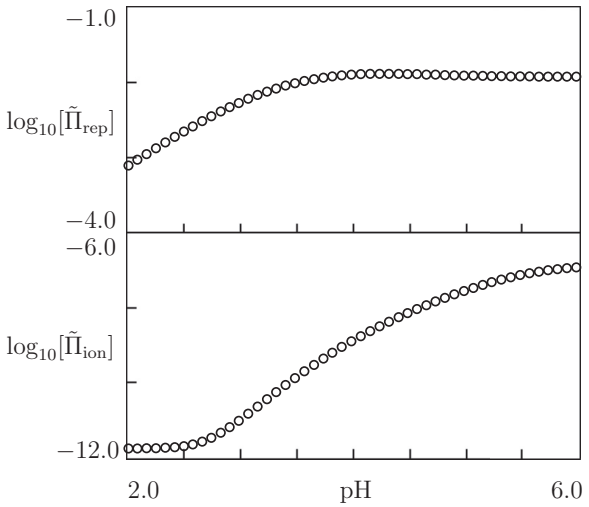

FIG. 12. Pressure driven by repulsion of charges $\tilde{\Pi}_{\rm rep}$ and ionic pressure $\tilde{\Pi}_{\rm ion}$ versus pH. Circles: results of simulation for AAc gel.

Substitution of Eqs. (70), (95), and (96) into Eq. (39) implies that

$$\mathbf{F}_e = \frac{1}{(1 + q_0 + q_1 C_b \alpha)^{\frac{1}{3}}} \times [\mathbf{e}_1 \otimes \mathbf{e}_1 + (1 + Cv)^{\frac{1}{2}}(\mathbf{e}_2 \otimes \mathbf{e}_2 + \mathbf{e}_3 \otimes \mathbf{e}_3)]. \tag{97}$$

It follows from Eqs. (43), (87), and (97) that

$$\mathbf{T} = T_1 \mathbf{e}_1 \otimes \mathbf{e}_1 + T(\mathbf{e}_2 \otimes \mathbf{e}_2 + \mathbf{e}_3 \otimes \mathbf{e}_3),$$

where

$$T_1 = -\Pi + \frac{G}{1 + Cv}\left[\frac{1}{(1 + q_0 + q_1 C_b \alpha)^{\frac{2}{3}}} - 1\right],$$

$$T = -\Pi + \frac{G}{1 + Cv}\left[\frac{1 + Cv}{(1 + q_0 + q_1 C_b \alpha)^{\frac{2}{3}}} - 1\right].$$

Bearing in mind that $T = 0$ for a cylinder with a traction-free lateral surface, we find that

$$\Pi = \frac{G}{1 + Cv}\left[\frac{1 + Cv}{(1 + q_0 + q_1 C_b \alpha)^{\frac{2}{3}}} - 1\right].$$

Inserting this expression into Eq. (84) and using Eqs. (82), (90), we obtain

$$\ln \frac{Q}{1 + Q} + \frac{1}{1 + Q} + \frac{\chi}{(1 + Q)^2} + \frac{g}{1 + Q}\left[\frac{1 + Q}{(1 + q_0 + \bar{q} Q_b \alpha)^{\frac{2}{3}}} - 1\right] - \frac{1}{X}\left(X - \frac{1}{\kappa} 10^{-p\mathrm{H}}\right)^{-2} = 0. \tag{98}$$

We analyze swelling diagrams on poly(2-hydroxyethyl methacrylate)-acrylic acid (HEMA-AAc) gels prepared by photopolymerization of a solution of monomers in water (molar ratio, 4:1) with 1 wt% of ethylene glycol dimethacrylate as a cross-linker [42]. Dry cylindrical specimens 180 μm long with diameters d_0 ranging from 300 to 700 μm were swollen in solutions of salts (monosodium phosphate and

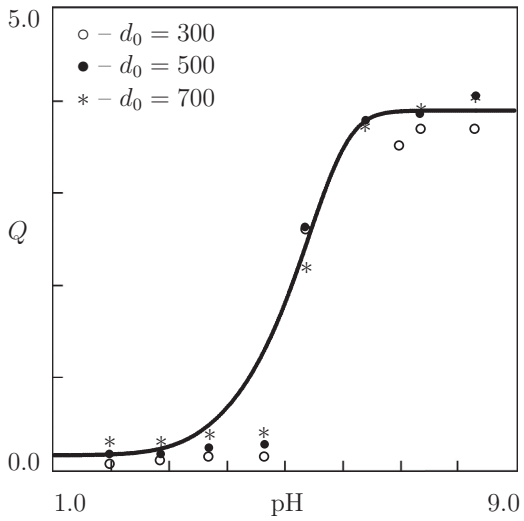

FIG. 13. Degree of swelling Q versus pH. Symbols: experimental data on HEMA-AAc gel samples with various initial diameters d_0 (in μm) [42]. Solid line: results of simulation.

sodium chloride) in water with an ionic strength 0.3 M. At each pH, the diameter d of a specimen in the fully swollen state was measured, and the degree of swelling Q was calculated as $Q = (d/d_0)^2 - 1$. Changes in degree of swelling are illustrated in Fig. 13, where Q is plotted versus pH for samples with $d_0 = 300$, 500, and 700 μm.

To approximate the data, Eqs. (83) and (98) are solved numerically by the Newton-Raphson algorithm. Calculations are conducted with $\chi = 0.4$, $q_0 = -0.99$, and $Q_b = 10^{-7}$. The dimensionless modulus $g = 0.04$ is determined by matching the data at low pH. The parameters $p\mathrm{K_a} = 5.9$ and $\bar{q} = 6.8 \times 10^7$ are found by fitting observations at high pH. The fact that $p\mathrm{K_a}$ exceeds its value for AAc in water is explained by the presence of salt in the buffer solution. Figure 13 demonstrates that Eqs. (83) and (98) ensure the same accuracy of matching

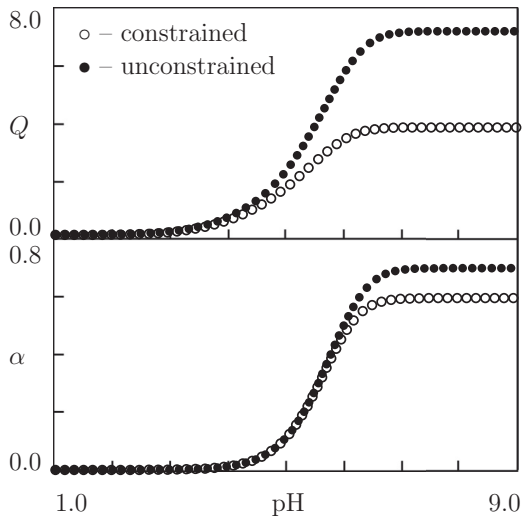

FIG. 14. Degree of swelling Q and degree of ionization α versus pH. Symbols: results of simulation for HEMA-AAc gel under constrained and unconstrained swelling.

observations as models with larger numbers of adjustable parameters [20,23,42].

To examine the effect of constraints on the degree of swelling Q and degree of ionization α, Eqs. (83), (91), and (98) are solved numerically with the material constants found by fitting observations in Fig. 13. Results of simulation are reported in Fig. 14, which demonstrates that the presence of constraints leads to a strong decay in the degree of swelling and a noticeable decrease in the degree of ionization at high pH, but weakly affects these quantities at low pH.

IV. CONCLUSIONS

A model is developed for the elastic response of a polyelectrolyte gel subjected to swelling. The gel is treated as a three-phase medium consisting of a solid phase (polymer network), a solvent (water), and solutes (mobile ions). Transport of solvent and solutes is modeled as their diffusion through the network accelerated by an electric field formed by mobile and fixed ions and accompanied by dissociation of functional groups attached to polymer chains. Constitutive equations are derived by means of the free energy imbalance inequality for an arbitrary three-dimensional deformation with finite strains. An advantage of this approach is that the Henderson-Hasselbach equation for degree of ionization of chains [with Eq. (66) providing the physical meaning of the dissociation constant] and van't Hoff formula for ionic pressure are not postulated phenomenologically, but are developed together with other constitutive relations.

In the analysis of equilibrium swelling diagrams, both ionic pressure and electrostatic interaction of bound charges are taken into account. To describe electrostatic repulsion of fixed ions in a tractable way, the reference (stress-free) state of the equivalent polymer network is presumed to differ from the initial state of a dry undeformed gel, and the coefficient of volume expansion of the equivalent network is treated as a linear function of the degree of ionization of chains.

The model is applied to study unconstrained and constrained swelling of gels in a water bath with various pH's. Analysis of swelling diagrams is performed within the concept of Donnan equilibrium. The governing equations involve six adjustable parameters, which are found by matching observations on DMA-IAc, AA-IAc, PVA-AsAc, and HEMA-AAc composite hydrogels. Numerical analysis reveals that (i) the model ensures good agreement between experimental data and results of simulation (Figs. 1, 3, 4, 7, 11, and 13), (ii) the material parameters change consistently with the composition of hydrogels (Figs. 2, 5, and 8), and (iii) the governing equations describe observations without adjustment of the dissociation constant and employment of the Flory-Huggins parameter that exceeds $\frac{1}{2}$ [14,43].

Numerical analysis demonstrates that the osmotic pressure Π_{rep} induced by electrostatic repulsion of bound charges plays an important role in water uptake by polyelectrolyte gels. This quantity (disregarded in some conventional models) exceeds the ionic pressure Π_{ion} calculated by means of the van't Hoff law by several orders of magnitude. Among other results, it is worth noting the strong decrease in the degree of swelling at high pH accompanied by a reduction in the degree of ionization when geometric constraints are imposed on a gel specimen.

The following limitations of the constitutive model should be mentioned. (i) Reaction-diffusion equations, (35), do not discriminate vehicular motion of ions and Grotthuss shuttling [44]. (ii) The linear relation, (70), between the coefficient of volume expansion of the equivalent network f and the degree of ionization α is valid at low concentrations of mobile ions only. This equation should be corrected for polyampholyte gels and for polyelectrolyte gels in solutions of salts (the Manning condensation). (iii) Equation (46) for the free energy density is incomplete for ionic strength-sensitive gels, as it does not account for the energies of mixing of mobile ions [12] and formation of ion pairs [45].

ACKNOWLEDGMENT

Financial support by the European Commission through FP7-NMP programme (Project 314744) is gratefully acknowledged.

APPENDIX

Substitution of Eqs. (47)–(50) into Eq. (46) implies that

$$\begin{aligned}\Psi = {}& \mu^0 C + k_B T C\left(\ln\frac{Cv}{1+Cv} + \frac{\chi}{1+Cv}\right) + \mu^0_{\mathrm{H}^+} C_{\mathrm{H}^+} + k_B T C_{\mathrm{H}^+}\left(\ln\frac{C_{\mathrm{H}^+}}{C} - 1\right)\\ &+ \mu^0_{\mathrm{OH}^-} C_{\mathrm{OH}^-} + k_B T C_{\mathrm{OH}^-}\left(\ln\frac{C_{\mathrm{OH}^-}}{C} - 1\right) + \mu^0_{\mathrm{Cl}^-} C_{\mathrm{Cl}^-} + k_B T C_{\mathrm{Cl}^-}\left(\ln\frac{C_{\mathrm{Cl}^-}}{C} - 1\right)\\ &+ k_B T C_{\mathrm{b}}[\alpha\ln\alpha + (1-\alpha)\ln(1-\alpha)] + W + W_{\mathrm{el}}. \end{aligned} \tag{A1}$$

The derivative of Eq. (48) with respect to time reads

$$\dot W = W_{,1}\dot J_{e1} + W_{,2}\dot J_{e2} + W_{,3}\dot J_{e1} + W_{,\alpha}\dot\alpha + W_{,f}\dot f,$$

where

$$W_{,m} = \frac{\partial W}{\partial J_{em}}, \quad W_{,\alpha} = \frac{\partial W}{\partial \alpha}, \quad W_{,f} = \frac{\partial W}{\partial f}.$$

It follows from this relation and Eq. (45) that

$$\dot W = 2\mathbf{K}_{\mathrm{mech}} : \mathbf{D} + W_{,\alpha}\dot\alpha - \left(\frac{2K}{3f} - W_{,f}\right)\dot f, \tag{A2}$$

where

$$\mathbf{K}_{\mathrm{mech}} = W_{,1}\mathbf{B}_e - J_{e3}W_{,2}\mathbf{B}_e^{-1} + (J_{e2}W_{,2} + J_{e3}W_{,3})\mathbf{I}, \quad K = J_{e1}W_{,1} + 2J_{e2}W_{,2} + 3J_{e3}W_{,3}. \tag{A3}$$

Differentiating Eq. (25) with respect to time and using Eq. (23), we find that

$$\dot W_{\mathrm{el}} = \mathbf{E}\cdot\dot{\mathbf{H}} + \frac{1}{2\epsilon J}\left(\mathbf{H}\cdot\dot{\mathbf{C}}\cdot\mathbf{H} - \frac{\dot J}{J}\mathbf{H}\cdot\mathbf{C}\cdot\mathbf{H}\right). \tag{A4}$$

It follows from Eqs. (8), (41), and (42) that

$$\dot{\mathbf{C}} = 2\mathbf{F}^\top\cdot\mathbf{D}\cdot\mathbf{F}.$$

Combination of this equality with Eq. (23) yields

$$\frac{1}{2\epsilon J}\mathbf{H}\cdot\dot{\mathbf{C}}\cdot\mathbf{H} = \frac{1}{\epsilon J}\mathbf{H}\cdot\mathbf{F}^\top\cdot\mathbf{D}\cdot\mathbf{F}\cdot\mathbf{H} = \frac{J}{\epsilon}\mathbf{h}\cdot\mathbf{D}\cdot\mathbf{h} = \frac{J}{\epsilon}(\mathbf{h}\otimes\mathbf{h}) : \mathbf{D}, \tag{A5}$$

where $\otimes$ stands for the tensor product. Keeping in mind that

$$\dot J = J\mathbf{I} : \mathbf{D} \tag{A6}$$

and utilizing Eq. (8), we conclude that

$$\frac{\dot J}{2\epsilon J^2}\mathbf{H}\cdot\mathbf{C}\cdot\mathbf{H} = \frac{1}{2\epsilon J}\mathbf{H}\cdot\mathbf{F}^\top\cdot\mathbf{F}\cdot\mathbf{H}(\mathbf{I} : \mathbf{D}) = \frac{J}{2\epsilon}(\mathbf{h}\cdot\mathbf{h})\mathbf{I} : \mathbf{D}. \tag{A7}$$

Substitution of Eqs. (A5) and (A7) into Eq. (A4) implies that

$$\dot W_{\mathrm{el}} = \mathbf{E}\cdot\dot{\mathbf{H}} + 2\mathbf{K}_{\mathrm{el}} : \mathbf{D}, \tag{A8}$$

where

$$\mathbf{K}_{\rm el} = \frac{J}{2\epsilon}\left[(\mathbf{h}\otimes\mathbf{h}) - \frac{1}{2}(\mathbf{h}\cdot\mathbf{h})\mathbf{I}\right]. \tag{A9}$$

Differentiating Eq. (A1) with respect to time and using Eqs. (A2) and (A8), we arrive at Eq. (56) with

$$\begin{aligned}
\Theta_C &= \mu^0 + k_B T\left[\ln\frac{Cv}{1+Cv} + \frac{1}{1+Cv} + \frac{\chi}{(1+Cv)^2} - \frac{C_{\rm H^+}+C_{\rm OH^-}+C_{\rm Cl^-}}{C}\right],\\
\Theta_{\rm H^+} &= \mu^0_{\rm H^+} + k_B T\ln\frac{C_{\rm H^+}}{C}, \quad \Theta_{\rm OH^-} = \mu^0_{\rm OH^-} + k_B T\ln\frac{C_{\rm OH^-}}{C},\\
\Theta_{\rm Cl^-} &= \mu^0_{\rm Cl^-} + k_B T\ln\frac{C_{\rm Cl^-}}{C}, \quad \Theta_\alpha = k_B T\ln\frac{\alpha}{1-\alpha}.
\end{aligned} \tag{A10}$$

[1] S. Van Vlierberghe, P. Dubruel, and E. Schacht, Biomacromolecules **12**, 1387 (2011).
[2] S.-K. Ahn, R. M. Kasi, S.-C. Kim, N. Sharma, and Y. Zhou, Soft Matter **4**, 1151 (2008).
[3] J. Hu, G. Zhang, and S. Liu, Chem. Soc. Rev. **41**, 5933 (2012).
[4] E. M. White, J. Yatvin, J. B. Grubbs, J. A. Bilbrey, and J. Locklin, J. Polym. Sci. B: Polym. Phys. **51**, 1084 (2013).
[5] M. A. C. Stuart, W. T. S. Huck, J. Genzer, M. Muller, C. Ober, M. Stamm, G. B. Sukhorukov, I. Szleifer, V. V. Tsukruk, M. Urban, F. Winnik, S. Zauscher, I. Luzinov, and S. Minko, Nat. Mater. **9**, 101 (2010).
[6] R. Messing and A. M. Schmidt, Polym. Chem. **2**, 18 (2011).
[7] D. Buenger, F. Topuz, and J. Groll, Progr. Polym. Sci. **37**, 1678 (2012).
[8] C. Alvarez-Lorenzo and A. Concheiro, Chem. Commun. **50**, 7743 (2014).
[9] E. Kokufuta, Langmuir **21**, 10004 (2005).
[10] S. Mafe, J. A. Manzanares, A. E. English, and T. Tanaka, Phys. Rev. Lett. **79**, 3086 (1997).
[11] A. V. Dobrynin and J.-M. Y. Carrillo, J. Phys.: Condens. Matter **21**, 424112 (2009).
[12] G. S. Longo, M. Olvera de la Cruz, and I. Szleifer, Macromolecules **44**, 147 (2011).
[13] J. Hua, M. K. Mitra, and M. Muthukumar, J. Chem. Phys. **136**, 134901 (2012).
[14] R. Marcombe, S. Cai, W. Hong, X. Zhao, Y. Lapusta, and Z. Suo, Soft Matter **6**, 784 (2010).
[15] M. Quesada-Perez, J. A. Maroto-Centeno, J. Forcada, and R. Hidalgo-Alvarez, Soft Matter **7**, 10536 (2011).
[16] S. Baek and A. R. Srinivasa, Int. J. Non-Lin. Mech. **39**, 1301 (2004).
[17] H. Li, R. Luo, E. Birgersson, and K. Y. Lam, J. Appl. Phys. **101**, 114905 (2007).
[18] L. Feng, Y. Jia, X. Chen, X. Li, and L. An, J. Chem. Phys. **133**, 114904 (2010).
[19] W. Hong, X. Zhao, and Z. Suo, J. Mech. Phys. Solids **58**, 558 (2010).
[20] T. Y. Ng, H. Li, and Y. K. Yew, Int. J. Solids Struct. **47**, 614 (2010).
[21] J. P. Keener, S. Sircar, and A. L. Fogelson, Phys. Rev. E **83**, 041802 (2011).
[22] T. Wallmersperger, K. Keller, B. Kroplin, M. Gunther, and G. Gerlach, Colloid Polym. Sci. **289**, 535 (2011).
[23] J. C. Kurnia, E. Birgersson, and A. S. Mujumdar, Polymer **53**, 613 (2012).
[24] S. Sircar, J. P. Keener, and A. L. Fogelson, J. Chem. Phys. **138**, 014901 (2013).
[25] H. Yan and B. Jin, Eur. Phys. J. E **36**, 27 (2013).
[26] J. Li, Z. Suo, and J. J. Vlassak, Soft Matter **10**, 2582 (2014).
[27] P. E. Grimshaw, J. H. Nussbaum, A. J. Grodzinsky, and M. L. Yarmush, J. Chem. Phys. **93**, 4462 (1990).
[28] K. Kamran, M. van Soestbergen, H. P. Huinink, and L. Pel, Electrochim. Acta **78**, 229 (2012).
[29] P. Nardinocchi, M. Pezzula, and L. Placidi, J. Intell. Mater. Syst. Struct. **22**, 1887 (2011).
[30] P. J. Flory, J. Chem. Phys. **10**, 51 (1942).
[31] M. L. Huggins, J. Chem. Phys. **9**, 440 (1941).
[32] R. Bustamante, A. Dorfmann, and R. W. Ogden, Int. J. Eng. Sci. **47**, 1131 (2009).
[33] A. D. Drozdov, Int. J. Appl. Mech. **6**, 1450023 (2014).
[34] A. D. Drozdov and J. de C. Christiansen, Int. J. Solids Struct. **50**, 1494 (2013).
[35] A. D. Drozdov and J. de C. Christiansen, Int. J. Solids Struct. **50**, 3570 (2013).
[36] J. Ricka and T. Tanaka, Macromolecules **17**, 2916 (1984).
[37] D. Capriles-Gonzalez, B. Sierra-Martin, A. Fernandez-Nieves, and A. Fernandez-Barbero, J. Phys. Chem. B **112**, 12195 (2008).
[38] T. Celik and N. Orakdogen, J. Mater. Res. **28**, 3234 (2013).
[39] H. Schurmans, H. Thun, and F. Verbeek, J. Electroanal. Chem. Interf. Electrochem. **26**, 299 (1970).
[40] M. Liu, L. Wang, H. Su, H. Cao, and T. Tan, Polym. Bull. **70**, 2815 (2013).
[41] S. Naficy, J. M. Razal, P. G. Whitten, G. G. Wallace, and G. M. Spinks, J. Polym. Sci. Part B: Polym. Phys. **50**, 423 (2012).
[42] S. K. De, N. R. Atluri, B. Johnson, W. C. Crone, D. E. Beebe, and J. Moore, J. Microelectromech. Syst. **11**, 544 (2002).
[43] V. Torma, T. Gyenes, Z. Szakacs, and M. Zrinyi, Acta Biomater. **6**, 1186 (2010).
[44] N. Agmon, Chem. Phys. Lett. **244**, 456 (1995).
[45] C. E. Sing, J. W. Zwanikken, and M. Olvera de la Cruz, Macromolecules **46**, 5053 (2013).